Petroleum Science 19 (2022) 608–618

Contents lists available at ScienceDirect

Petroleum Science

journal homepage: www.keaipublishing.com/en/journals/petroleum-science

Original Paper

Notoginsenoside as an environmentally friendly shale inhibitor in water-based drilling fluid

Jin-Sheng Sun [a, b, *], Zong-Lun Wang [a, b], Jing-Ping Liu [a, b], Kai-He Lv [a, b], Fan Zhang [a, b], Zi-Hua Shao [a, b], Xiao-Dong Dong [a, b], Zhi-Wen Dai [a, b], Xian-Fa Zhang [a, b]

[a] College of Petroleum Engineering, China University of Petroleum (East China), Qingdao, 266580, Shandong, People's Republic of China
[b] Key Laboratory of Unconventional Oil & Gas Development (China University of Petroleum (East China)), Ministry of Education, Qingdao, 266580, Shandong, People's Republic of China

ARTICLE INFO

Article history:
Received 6 April 2021
Accepted 15 November 2021
Available online 20 November 2021

Edited by Yan-Hua Sun

Keywords:
Notoginsenoside
Shale inhibition
Environmentally friendly
Water-based drilling fluid
Inhibition mechanism

ABSTRACT

The demand for non-toxic and biodegradable shale inhibitors is growing in the drilling industry. In this paper, the effect of notoginsenoside (NS) as a new, environmentally friendly inhibitor of shale hydration is systematically studied for the first time. The inhibition performance of NS was evaluated via inhibition evaluation tests, including mud ball immersion tests, linear expansion tests, shale rolling recovery tests, and compressive strength tests. The inhibition mechanism of NS was analyzed using Fourier transform infrared spectroscopy (FTIR), contact angle measurements, particle size distribution determination, thermogravimetric analysis (TGA), and scanning electron microscopy (SEM). The experimental results demonstrate that NS is able to adhere to the clay surface, forming a hydrophobic film that prevents the entry of water molecules and inhibiting the hydration dispersion of the clay. Because of this, NS can maintain the original state of bentonite pellets in water, which can effectively reduce the swelling rate of bentonite, increase the recovery rate of shale drill cuttings, maintain the strength of the shale, and therefore maintain the stability of the borehole wall during drilling. In addition, NS is non-toxic, degradable, and compatible with water-based drilling fluids. The above advantages make NS a promising candidate for use as an environmentally friendly shale inhibitor.

1. Introduction

Shale gas has attracted an increasing amount of attention in recent years because it has a lower carbon content (Salkuyeh and Adams II, 2015) and generates less pollution (Estrada and Bhamidimarri, 2016; Zhang et al., 2018) than conventional fossil fuels (e.g., coal and oil). However, shale gas reservoirs in China are generally deeply buried with high water sensitivity under complex geological conditions where fracture is easily induced. The drilling fluid infiltrates along the fractures, and mechanical and physical-chemical interactions occur with the formation rock, resulting in a decrease in the rock strength, a change in the stress state near the wellbore, and thus wellbore instability (Chen et al., 2003; Lal, 1999; Li et al., 2015; Pašić et al., 2007; Yu et al., 2003). Shale wellbore instability is partly caused by the hydration expansion and dispersion of the water-sensitive clay in mud shale (Talabani et al., 1993). At present, the most common way to solve this problem is to use oil-based drilling fluid, which typically provides satisfactory borehole stability and has a strong suppression capacity. However, oil-based drilling fluids are generally expensive and usually result in pollution (Wei et al., 2016; Zhong et al., 2014). The development of an economical and environmentally friendly drilling fluid has become one of the main research directions in the oil and gas industry. Researchers have developed synthetic drilling fluid to replace oil-based drilling fluid, which reduces the impact on the environment and ensures the high inhibition ability of traditional oil-based drilling fluids (Li et al. 2016a, 2016b, 2019; Razali et al., 2018; van Oort et al., 2004). However, its high cost limits the development of synthetic based drilling fluid. And the availability of high-performance water-based drilling fluid not only greatly reduces the performance gap with oil-based drilling fluid but also achieves low cost and environmental protection (Aftab et al., 2020; Dye et al., 2005; Patel et al., 2007).

* Corresponding author. College of Petroleum Engineering, China University of Petroleum (East China), Qingdao, 266580, Shandong, People's Republic of China.
E-mail address: sunjsdri@cnpc.com.cn (J.-S. Sun).

https://doi.org/10.1016/j.petsci.2021.11.017

One of the cores of high-performance water-based drilling fluids is the development of a shale inhibitor. Currently, a series of shale inhibitors have been developed. For example, once KCl (Boek et al., 1995; O'Brien and Chenevert, 1973) enters the crystal layer of clay, the potassium ions can form a tight structure with the clay, preventing the clay to hydrate and disperse. Once a polyamine (PA) inhibitor (Peng et al., 2013; Qu et al., 2009; Zhong et al., 2016) with positive charges enters the clay layer space and adsorbs onto the clay with negative charges through electrostatic interaction, the adjacent clay layer structures will be combined together, which hinders the invasion of water molecules to hydrate the clay. Polymer-based inhibitors (Bai et al., 2017; Jiang et al., 2016; Liu et al., 2014) reduce the hydration of shale by bridging the adsorption among clay slices and forming polymer films on clay surfaces to stabilize the shale. Surfactants (Liu et al., 2019; Moslemizadeh et al., 2016; Shadizadeh et al., 2015) inhibit shale hydration by forming a hydrophobic film on the clay surfaces to prevent water from entering. Moreover, with the development of nanotechnology, nano-materials have also been used to stabilize borehole walls (Cai et al., 2012; Hoelscher et al., 2012; Huang et al. 2018a, 2018b; Spisak, 2011). However, these inhibitors still have some disadvantages, such as negative environmental impacts and poor inhibition effects, so it is urgent to develop a new type of inhibitor that is environmentally friendly and has a better inhibition effect.

Panax notoginseng is a type of ginseng plant in the Acanthopanax family. It is a commonly used hemostatic, blood activating, and blood tonifying medicinal material. It is widely found in Jiangxi, Hubei, Guangdong, Yunnan, Guizhou, Sichuan, Myanmar, Bhutan, and other places, with a rich yield and output value of 100 billion yuan (Wang et al. 2006, 2016; Xu et al., 2019). Notoginsenoside (NS) is the main active ingredient of Panax notoginseng, which is mainly used for promoting blood circulation, removing blood stasis, dredging channels, and activating collaterals. Studies have shown that NS has been widely used in medical research and applications, such as atherosclerosis, diabetes, and cardiovascular and cerebrovascular diseases (Duan et al., 2017; Qu et al., 2020; Uzayisenga et al., 2014; Yang et al., 2014). But to the best of our knowledge, there is almost no literature concerning the use of NS as a shale inhibitor. In this study, we systematically studied its effect as an inhibitor in shale well drillings and analyzed its inhibition mechanism. It was found that NS demonstrates a promising inhibition effect on shale hydration. This study provides a new environmentally friendly method of inhibiting shale hydration.

2. Experimental

2.1. Materials

The notoginsenoside (NS, 80% purity) was obtained from Xi'an Prius Biological Engineering Co., Ltd. The properties of NS are presented in Table 1. Notoginsenoside is a natural biosurfactant. The molecular structure of NS is shown in Fig. 1. Its saponin molecular structure is amphiphilic, the hydrophobic part is dammarane in triterpenoid saponin, and the hydrophilic part is composed of sugar chains. The polyamine (PA) inhibitor is a type of polyether amine, which is obtained by amination of polypropylene glycol under high-temperature and high-pressure conditions. FA-367 is a zwitterionic polymer thickening coating agent. CMJ-2 is a cationic lignite anti-collapse fluid loss agent. PAC-LV is a polyanionic cellulose fluid loss agent. NP-1 is a nano-polyester plugging agent. The potassium chloride and sodium carbonate were provided by Aladdin Pharmaceutical Co., Ltd. The FA-367 and PA were purchased from Shandong Juxin Chemical Co., Ltd. The CMJ-2 and PAC-LV were provided by the Anhui Luhai Oil Additives Technology Co., Ltd. The NP-1 and emulsified asphalt were obtained from the Shandong Deshunyuan Petroleum Technology Co., Ltd. The barite was obtained from the Anxian Huaxi Mineral Powder Co., Ltd. The sodium bentonite was provided by the Huaian Drilling Co., and the shale cuttings were obtained from the Chuanqing Drilling Co. The mineral composition of the shale samples was analyzed using X-ray diffraction (XRD-6100, Shimadzu Corp.) (Table 2).

Table 1
Properties of the NS extract.

Product	Property
Used part	Notoginseng
Description	Fine powder
Color	Yellow
Solubility in cold water	Soluble
Solubility in alcohol	Soluble
Molecular weight	300–500
Product model	5623

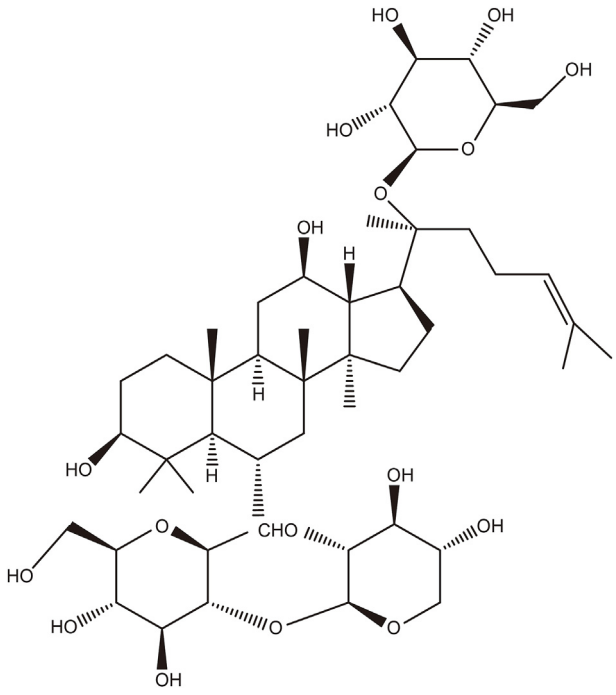

Fig. 1. Molecular structure of NS.

2.2. Mud ball immersion test

The mud ball immersion test is a widely used method of evaluating inhibition performance. A certain proportion of the constituents (the mass ratio of bentonite to distilled water is 2:1) was used to prepare the mud balls. These mud balls were immersed in different solutions (60 mL of distilled water (DI) and 3 wt% PA, 5 wt % KCl, 1 wt% NS, 2 wt% NS, or 3 wt% NS) for 24 h. Then the samples were checked for cracks or dilapidation (Chen et al., 2017; Lv et al., 2020; Zhang et al., 2019).

2.3. Linear swelling test

The linear swelling test can quantitatively evaluate the swelling of clay. In this test, 10 g of sodium bentonite (100 mesh sieve, 103 °C drying for 12 h) was pressurized to 10 MPa using a manual hydraulic pump in a mold. The pressure was maintained for 10 min in order to form artificial cores. The thickness of the core was measured and recorded as the initial thickness (H_0). The prepared

Table 2
Mineralogical composition of the shale samples.

Content, wt%							Relative content of clay minerals, wt%			
Quartz	Calcite	Pyrite	K-feldspar	Plagioclase	Dolomite	Clay minerals	Illite	Chlorite	Kaolinite	Illite/Smectite
40	6.7	4	2.2	2	3.8	38.2	27.9	16.2	1.9	49.9

artificial particles were set in contact with different solutions for 16 h in an HTP-C4-type double-channel shale dilatometer (Qingdao Tongchun Co., Ltd.). The relationship between the height variation (h) and time was monitored continuously (Xuan et al., 2013; Yang et al., 2017).

2.4. Shale cutting recovery test

The shale cutting recovery test is generally employed to examine the ability of a test solution to inhibit shale hydration, disintegration, and dispersion by analyzing the characteristics of the shale cuttings (Friedheim et al., 2011). In this test, the shale samples were crushed in a mineral crusher. The crushed shale particles were collected using sieves with sizes of 6–10 mesh. The prepared shale cuttings were dried at 103 °C in a constant-temperature oven for 10 h. A total of 50 g of shale cuttings and 350 mL of test fluids were added to a sealed pressure vessel and hot-rolled at 120 °C for 16 h in a rolling furnace. After cooling to ambient temperature, the remaining shale cuttings were screened with a 40-mesh sieve and washed with fresh water. The recovered shale cuttings were dried at 103 °C for 4 h before weighing. The recovery rate, which is the ratio of the initial sample weight to the final weight after the above procedures, was measured.

2.5. Shale compressive strength test

Significant attention has been devoted to the importance of shale strength during the drilling process. A lower shale strength is more likely to result in wellbore instability. In the shale compressive strength test, a shale core with a diameter of 25 mm and a length of 30 mm was dried at 105 °C for 4 h. After cooling to ambient temperature, a variety of inhibitors were added to solutions, and the shale cores were immersed in the solutions for 24 h (Huang et al., 2017). Then, the compressive strength was measured using a UTM5105X microcomputer controlled electronic universal testing machine (Shenzhen Sansizongheng Company, China).

2.6. Particle size distribution measurements

Clay material can be dispersed into tiny particles after hydration, even for a single unit of platelets. The particle size distribution of sodium bentonite can reflect its degree of hydration and inhibitory performance. A total of 14 g of sodium bentonite were added to 350 mL of DI water and were stirred for 2 h. The sample was then pre-hydrated for at least 24 h at room temperature. The dispersion was stirred for 12 h after the addition of the different dosages of the inhibitors. A small amount of the dispersion was diluted to a certain concentration to measure the particle size distribution. The particle size distribution of the dispersion was measured using a Mastersizer 3000 laser diffraction particle size analyzer (Malvern, UK) (Jia et al., 2019).

2.7. Adsorption measurements

First, 8.0 wt% sodium bentonite solution and 2 wt% NS solution were prepared. A total of 32 g of sodium bentonite were added to 400 mL of DI water and were stirred for 2 h. Then, the sample was pre-hydrated for at least 24 h at room temperature. The sodium bentonite solution was mixed with the NS solution in a ratio of 1:1. The mixture was placed in a constant temperature water bath oscillator at 25 °C and was oscillated for different amounts of time. After centrifugation (3000 rpm, 30 min) in a centrifuge, the supernatant was diluted and the organic carbon content was determined using a MultiN/C 2100 TOC/TN instrument (Jena Analytical Instrument Co., Ltd.). The adsorption capacity of the NS on the surface of the sodium bentonite was calculated, and the dynamic adsorption curve of NS and clay with time was plotted (Chu et al. 2019, 2020; Fu et al., 2020).

2.8. Fourier transform infrared spectroscopy (FTIR)

NS (2 g) was added to 100 mL of 2 wt% bentonite suspension and stirred at 300 rpm for 24 h. The NS-modified bentonite was centrifuged repeatedly and was dried. FTIR spectra of NS, bentonite, and NS-modified bentonite were analyzed using an IRTracer-100 infrared spectrometer (Shimadzu, Japan) at room temperature, with a wavenumber range of 400–4000 cm^{-1} and a resolution of 4 cm^{-1}.

2.9. Surface tension and contact angle measurements

The strong hydrophilicity of clay minerals is the driving factor of hydration expansion, which eventually leads to the instability of shale. Thus, the desired change in the hydrophilicity caused by shale-inhibitor interaction is beneficial to the stability of shale. In this experiment, the surface tensions and contact angles of a series of NS solutions with different concentrations were measured via the Washburn method (Edward, 1921, Xu et al., 2017) using a DCAT21 surface tension meter (Germany Data Physics Instrument Co., Ltd.). The modified shale cores were obtained by immersing in 1 wt% NS solution for 24 h and drying at 60 °C for 6 h. The contact angles of modified and unmodified shale cores were measured separately using an OCA-25 optical contact angle measuring instrument (German Data Co.).

2.10. Thermogravimetric analysis

In order to evaluate the effect of the NS concentration on the clay minerals, the thermal decomposition process of sodium bentonite modified using different NS concentrations and the original sodium bentonite was studied via thermogravimetric analysis (TGA). After 7 g of sodium bentonite was dispersed in 350 mL of DI water and stirred for 2 h, the dispersion was pre-hydrated for at least 24 h. Different concentrations of NS were added to the dispersion and were stirred for 12 h. The dispersion was centrifuged at 8000 rpm for 15 min and was washed with DI water three times. The precipitate was then collected. The precipitate was dried at 40 °C in preparation for the TGA using a simultaneous thermal analysis apparatus (TGA 550, Mettler Toldeo, USA).

2.11. Scanning electron microscopy

This test was performed to study the surface and microstructures of the shale before and after the NS modification. The

scanning electron microscopy (SEM) (Zeiss EVO MA 15/LS) was conducted to observe the ultrastructure. Sub-ion polished shale samples were placed in direct contact with 3 wt% NS solution for 24 h. These samples were labeled as modified shale samples after soaking. They were then dried in a vacuum drying chamber at 60 °C. Prior to the analysis, the samples were attached to an ion sputtering device for gold spraying in order to minimize the charging effect. Improvement of the imaging quality was made possible by the use of this methodology.

2.12. Scratch adhesion test

The scratch test has been widely used to test the adhesion between films and substrates (Chalker et al., 1991; Zhang et al., 2015). In the scratch test method, the indenter is slid across the film surface of the film substrate combination. In this process, the load L is continuously increased. When the critical value L_c (critical load) is reached, the film and the substrate begin to peel off, and the friction F between the indenter and the film substrate combination changes correspondingly. At this time, the brittle film will produce acoustic emissions. The acoustic emission peak is obtained at the critical load L_c on the acoustic emission signal load curve. The critical load L_c is the criterion for the adhesion between the film and the substrate (Attar and Johannesson, 1996; Bull and Berasetegui, 2006). The test samples were prepared according to the method described in Section 2.11. The adhesion between the membrane and shale was measured using an MFT-4000 multifunctional material surface performance tester (Lanzhou Huahui Instrument Technology Co., Ltd). The loading speed was 100 N/min, and the scratch length was 10 mm.

2.13. Environmental aspects

Drilling fluids abandoned during drilling operations can have negative impacts on the environment. The most effective way to minimize the impact of waste drilling fluids on the environment is to develop and implement environmentally friendly treatment agents. In addition to the performance of the treatment agent, the toxicity and biodegradability are also the main concerns determining the applicability of shale inhibitors in water-based drilling fluids. In this study, the 50% maximum effect concentration (EC_{50}), the chemical oxygen demand (COD), and the biochemical oxygen demand (BOD_5) of NS were used as the critical indicators (Chang et al., 2019; Ji et al., 2002; Pi et al., 2015). The evaluation methods are presented in Table 3.

2.14. Formulation optimization and performance evaluation of drilling fluid

Bentonite was added to water using an electric mixer to prepare a 4 wt% solution of the base drilling fluid, which was then cured at room temperature for 24 h. The filtration volume was measured at 30.0 min using a SD-3-type medium-pressure filtration apparatus (Qingdao Jiaonan Tongchun Machinery Petroleum instrument, China) by applying a pressure of 100±5 psi at 25.0 °C in accordance with the American Petroleum Institute (API) standards (Institute, 2009). The apparent viscosity (AV), plastic viscosity (PV), and yield point (YP) of the drilling fluid were tested according to the API standards under normal temperature and pressure conditions using a ZNN-D6 six-speed rotary viscometer (Qingdao Haitongda Special Instruments Co., Ltd.) (Huang et al., 2018a).

3. Results and discussion

3.1. Inhibition evaluation

3.1.1. Mud ball immersion tests

The immersion test results are shown in Fig. 2. After being immersed in water for 24 h, the volume of the mud ball expanded to the maximum degree, with large cracks appearing on the surface (Fig. 2a). The mud balls had a certain degree of cracking and expansion after being immersed in the 3 wt% PA and 5 wt% KCl water solutions (Fig. 2b and c). Interestingly, after being immersed in the NS solutions, the surfaces of the mud balls were smooth and intact, which demonstrates the apparent inhibition effect on swelling and cracking. In addition, the extent of the cracks on the surface of the clay ball decreased gradually and the inhibition effect improved with increasing NS concentration (Fig. 2d–f). The results of the mud ball experiments show that NS can effectively inhibit the hydration of mud balls, which may be due to the formation of an adsorption film on the surface of the mud ball, which prevents the water molecules from entering, thus inhibiting the hydration of the mud ball.

3.1.2. Linear swelling tests

The experimental results are shown in Fig. 3. The linear expansion rates of the sodium bentonite pellets in deionized water, 3 wt% PA, and 5 wt% KCl solution were 83.77%, 49.59%, and 66.80%, respectively. In the 1, 2, and 3 wt% NS solutions, the linear expansion rates were 55.98%, 42.95%, and 29.07%, respectively. The experimental results show that NS is able to suppress clay swelling and has a better performance than PA and KCl. As the NS concentration increases, the expansion rate decreases. This indicates that the inhibitory effect of NS increases with increasing concentration. These results demonstrate that NS can effectively prevent all water molecules from entering the clay and can inhibit the expansion of clay.

3.1.3. Shale cuttings recovery tests

Shale cuttings are clay-rich detritus generated in the drilling process, and the hot-rolling dispersion test was used to simulate the dispersion process of shale cuttings under drilling conditions. In this method, the higher recovery of shale cuttings after hot-rolling reflects the better inhibitive properties of the inhibitor. As shown in Fig. 4, the recovery of the shale cuttings in deionized water was 3.92%. After adding 5 wt% KCl, 3 wt% PA, 1 wt% NS, 2 wt% NS, and 3 wt% NS, the shale cuttings recovery increased to 15.63%, 19.26%, 18.35%, 36.24%, and 76.25%, respectively. These results show that the NS was able to inhibit shale cuttings dispersion and therefore performed better than KCl and PA. These results are consistent with those of the linear expansion tests.

Table 3
Methods of evaluating the NS environmental indicators.

Indicator	Method	National standard	Measuring instrument
EC_{50}	Luminescent bacteria	GB/T 18420.2-2009	Modern Water DeltaTox II
COD	Fast digestion spectrophotometric method	HJ/T 399-2007	LEICI-571 COD detector
BOD	Microbial electrode method	HJ557-2010HJ/T 86-2002	LY-05 BOD rapid measuring instrument

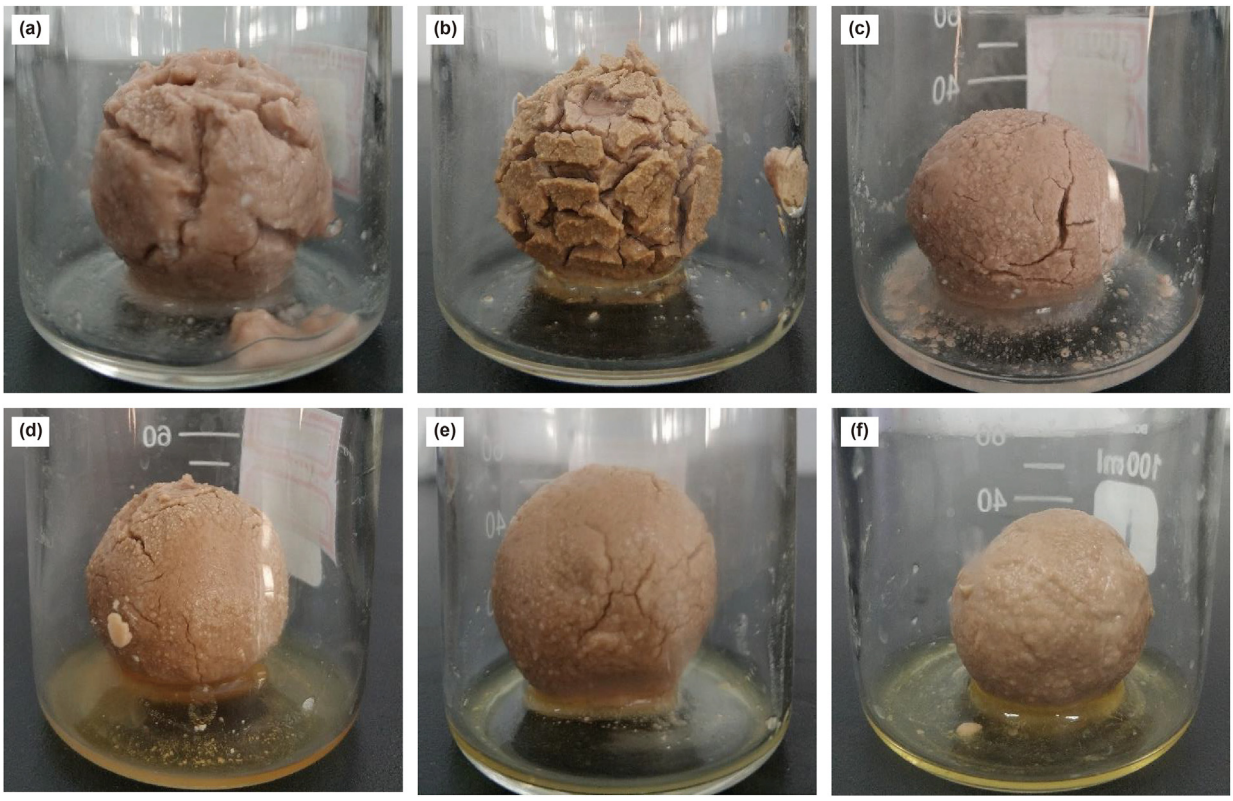

Fig. 2. Photographs of the mud balls after being immersed in (**a**) water, (**b**) 3 wt% PA, (**c**) 5 wt% KCl, (**d**) 1 wt% NS, (**e**) 2 wt% NS, and (**f**) 3 wt% NS for 24 h.

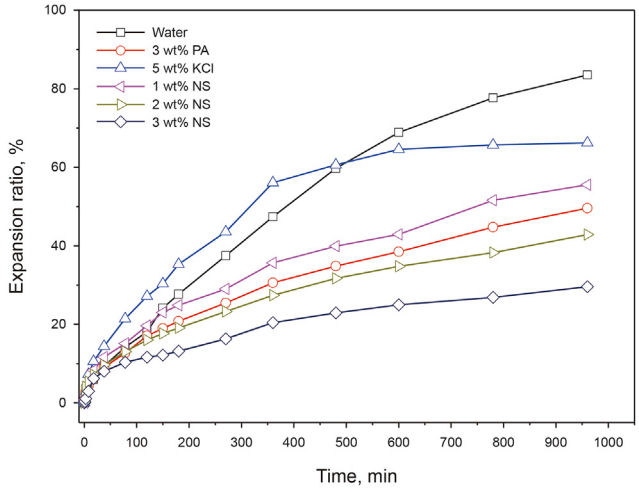

Fig. 3. Linear expansion rates of the tested inhibitors.

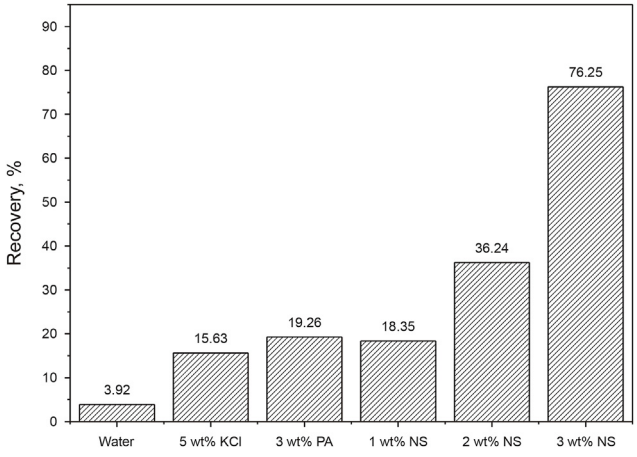

Fig. 4. Shale cuttings recovery rates of different inhibitors.

3.1.4. Shale compressive strength tests

As shown in Fig. 5, the compressive strength of the shale after soaking in water decreased from 157 MPa to 112 MPa, and adding inhibitors effectively improved the compressive strength of the shale. The effect of NS was better than those of PA and KCl. After adding 1 wt% NS, the compressive strength of the shale increased to 132 MPa, and with the increase in the NS concentration, the compressive strength of the shale continued to increase. When the concentration of NS reached 3 wt%, the compressive strength increased to 155 MPa, which was almost the same as that of the original shale. This is because the NS adhered to the shale surfaces, strengthening the wellbore and effectively maintained the strength of the shale.

3.1.5. Particle size distribution measurements

The differential and accumulative size distributions of the sodium bentonite for the addition of 5 wt% KCl, 3 wt% PA, 1 wt% NS, 2 wt% NS, and 3 wt% NS are shown in Fig. 6. The size of the sodium bentonite became larger in the presence of an inhibitor. It can be seen that the median particle size (d_{50}) of the sodium bentonite increased from 6.05 μm to 59.4 μm in deionized water in the presence of an inhibitor (Fig. 7). Among them, the effect of NS was better than those of PA and KCl, and the particle size of the sodium

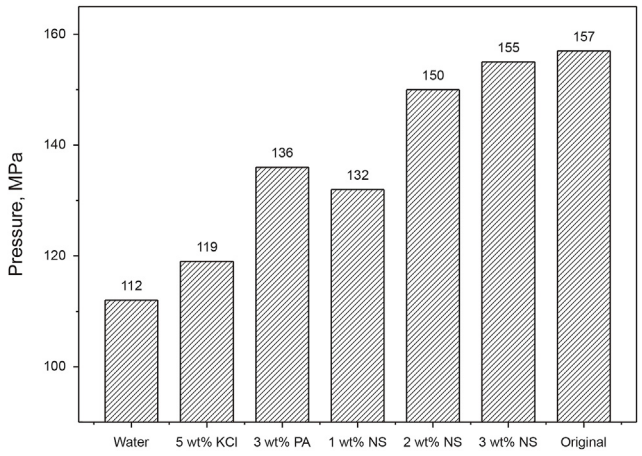

Fig. 5. Compressive strength of shale for different inhibitors.

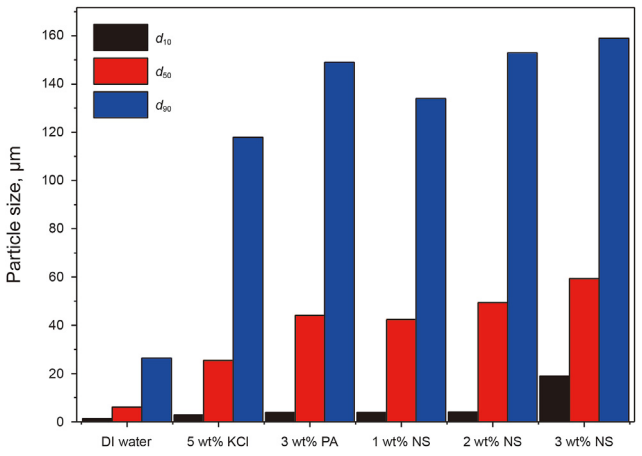

Fig. 7. Particle size distribution of sodium bentonite dispersion with different inhibitors.

bentonite increased with increasing NS concentration. This shows that NS can effectively inhibit the dispersion of clay particles and maintain the stability of shale cuttings, which was observed in the linear swelling tests (Fig. 3) and the shale cuttings recovery tests (Fig. 4).

3.2. Mechanism analysis

3.2.1. Adsorption behavior

The adsorption capacity of NS on Na-bentonite surfaces is shown in Fig. 8. It can be seen that the adsorption rate of NS on the bentonite surfaces is faster, the adsorption equilibrium can be reached in about 60 min, and the equilibrium adsorption capacity is 496.3 mg/g. The adsorption experiments show that NS can be rapidly adsorbed onto bentonite surfaces.

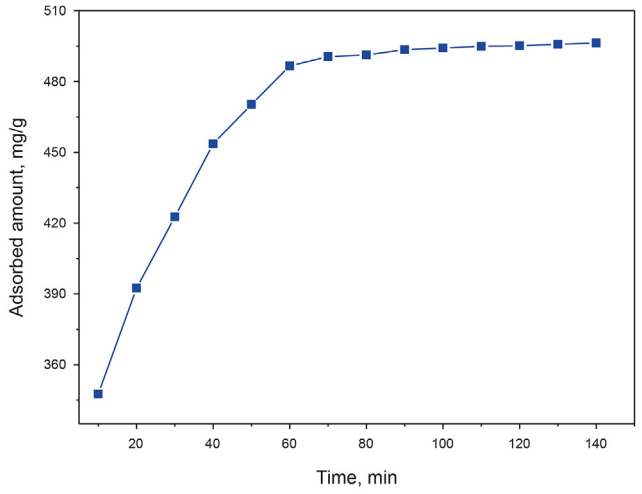

Fig. 8. Relationship between the adsorption capacity and adsorption time of NS on bentonite.

3.2.2. Adsorption mechanism analyzed via FTIR

Fig. 9 shows the FTIR spectrum of NS. A characteristic peak near 3389 cm^{-1} was confirmed as a tensile vibrational absorption peak of −OH. The characteristic peak near 2923 cm^{-1} of NS is the C−H bond tensile vibration peak in alkanes. The characteristic peak near 1665 cm^{-1} is identified as the tensile vibration peak of saturated fatty acid ester C═O. The characteristic peak near 1420 cm^{-1} is the bending vibration peak of the C−H bond in the alkane. The characteristic peak near 1044 cm^{-1} was identified as the characteristic peak of tensile vibration of C−O on the ether bond. The characteristic peak at 668 cm^{-1} was identified as the in-plane

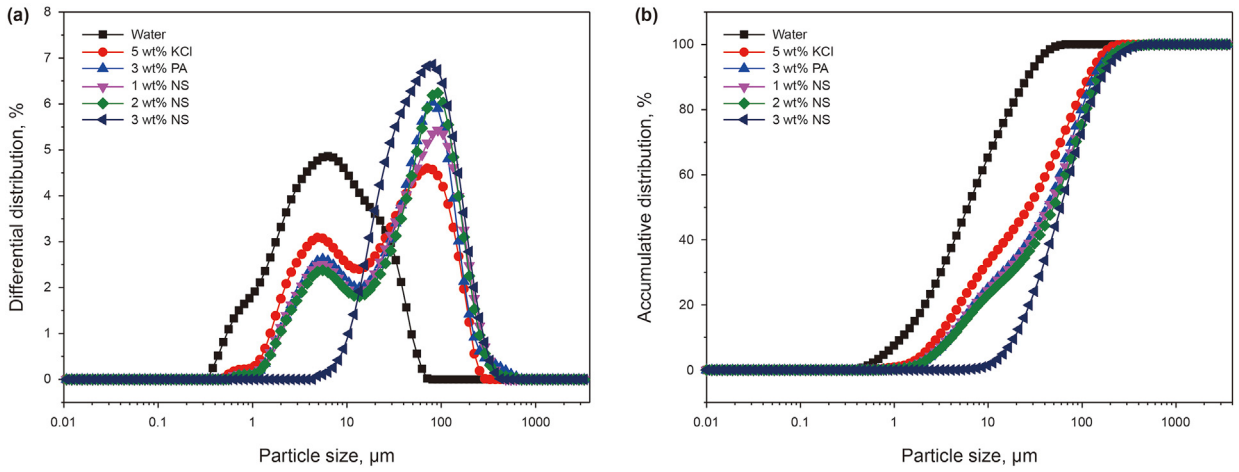

Fig. 6. Particle size distribution curves for sodium bentonite dispersion with different inhibitors.

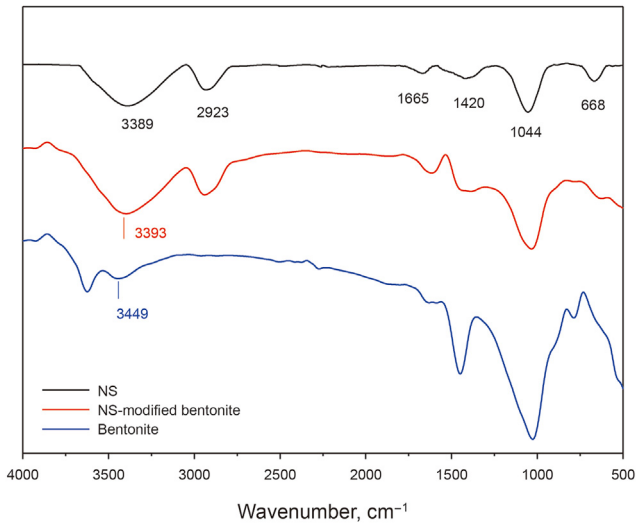

Fig. 9. FTIR spectra of bentonite, NS-modified bentonite, and NS.

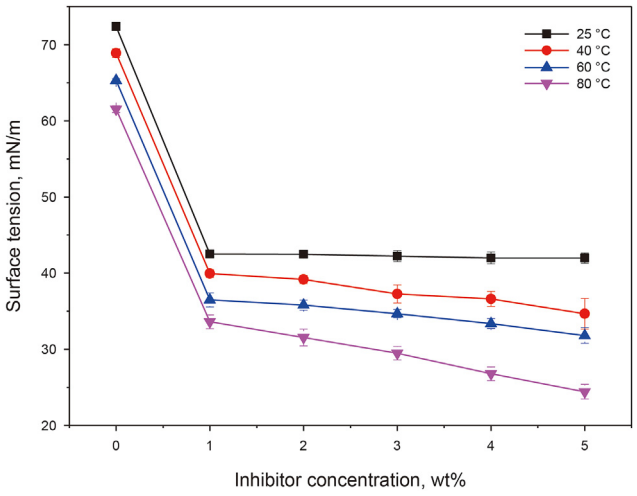

Fig. 10. Surface tension of the inhibitor at different concentrations and temperatures.

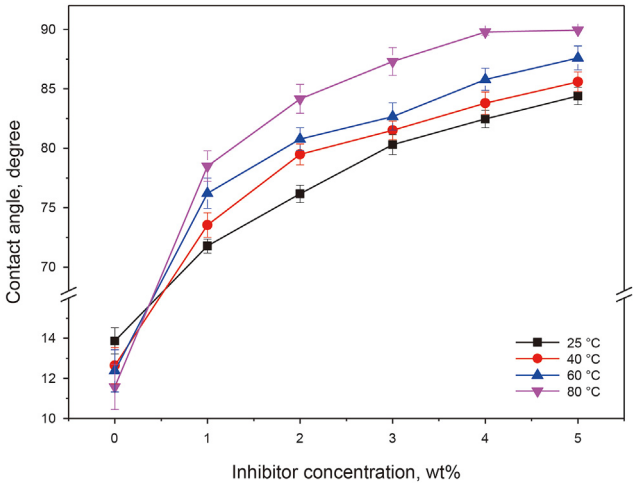

Fig. 11. Contact angle of the shale at different temperatures after immersion in water solutions containing different inhibitor concentrations.

and out-of-plane bending vibration characteristic peak of the −OH bond on the ring.

The FTIR spectra of bentonite and NS-modified bentonite confirm the hydrogen bond induced adsorption. As shown in Fig. 9, the peak at 3449 cm^{-1} in the FTIR spectrum of bentonite is caused by the tensile vibration of H−O−H (bound water of bentonite). After the NS adsorbed onto the bentonite, the wavenumber of the H−O−H stretching vibration (3449 cm^{-1}) red shifted to a lower number (3393 cm^{-1}). This is due to the longer H−O−H bond length of bentonite and the attraction (hydrogen bond) between the hydroxyl group of the NS and the H−O−H of bentonite. In this way, the stretching vibration frequency of H−O−H was reduced, resulting in the wavenumber of the H−O−H stretching being decreased. This shows that the NS was adsorbed onto the bentonite by hydrogen bond adsorption between the NS and the clay (Lv et al., 2020; Tabak et al., 2007).

3.2.3. Surface tension and contact angle measurements

The hydration of shale is related to its hydrophobicity. The stronger the hydrophobicity of the clay surface, the lower the affinity between the clay and water. Therefore, the interaction between the inhibitors and the shale can change its hydrophobicity, which can effectively maintain the stability of the shale. The surface tension and contact angle measurements for different concentrations of NS are shown in Figs. 10 and 11, respectively. The surface tension of the solution decreases with increasing NS concentration and with increasing temperature. The smallest surface tension was 23.35 mN/m at 80 °C. This shows that NS can effectively reduce the surface tension of water, thus reducing the capillary force of the shale and the water absorption caused by the capillary force. As the NS concentration increased, the contact angle of the shale increased from 13.2° (in fresh water) to 84.45° at 25 °C. As the temperature increased from 25 °C to 80 °C, the greatest contact angle increased to 89.89°. When the temperature increased, the contact angle between the shale and water increased. As the contact angle between the shale and water increased, the hydrophobicity of the shale increased, and the stability of the shale was effectively maintained. Fig. 12 also proves that the wettability of shale core surface has changed after NS modification. The contact angle of shale core modified by NS increased from 11.8° to 71.5°. This experiment shows that NS can change the wettability of the shale surface and prevent the entry of water molecules, thus inhibiting the hydration of the shale. This is consistent with the results of the mud ball experiments and the linear expansion, rolling recovery, and compressive strength tests.

3.2.4. TGA analysis

As shown in Fig. 13, the unmodified bentonite has two main stages of quality loss. The first stage is the loss of adsorbed water from the surface and the middle layer. The corresponding temperature is less than 110 °C. During this stage, the quality loss of the original bentonite was 7.39%. The mass loss of 1 wt% NS-modified bentonite during this stage was 4.37%, that of 2 wt% NS-modified bentonite was 1.91%, and that of 3 wt% NS-modified bentonite was 1.33%. The modified bentonite adsorbed less free water, and the water absorption rate varied as the concentration increased. The less free water in the middle layer, the weaker the swelling and dispersibility of the bentonite. These observations are consistent with the results of the linear expansion experiments (Fig. 3).

The second stage of weight loss occurred between 400 and 700 °C was attributed to structural (hydroxyl) water. The quality loss stage of the modified bentonite was significantly different from that of the original bentonite. When the temperature was less than 110 °C, the main mass loss of the modified bentonite was due to the

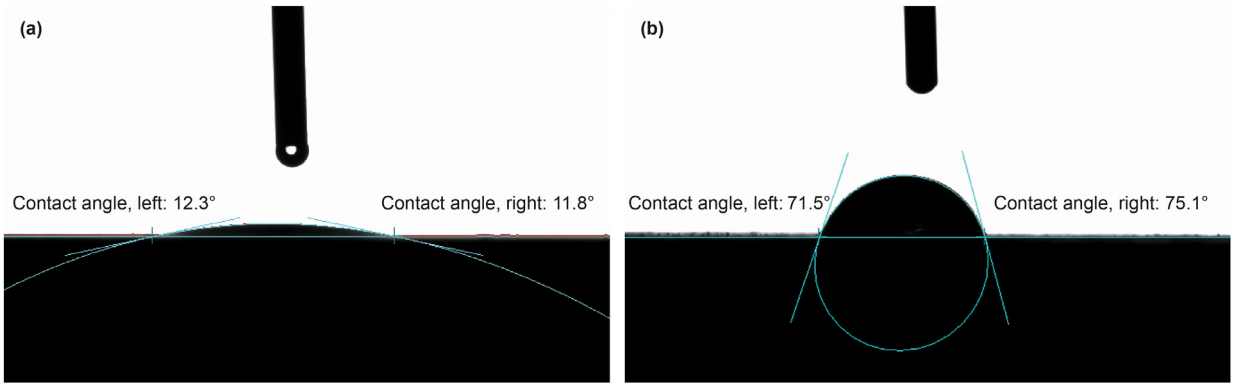

Fig. 12. Contact angle of shale cores: (**a**) unmodified shale core and (**b**) modified shale core after exposure to 1 wt% NS solution for 24 h.

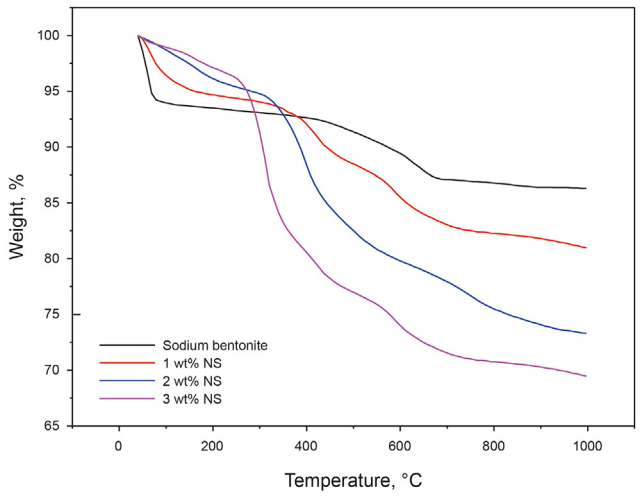

Fig. 13. TGA curves of sodium bentonite and modified sodium bentonite with different NS concentrations.

degradation of NS between 250 and 500 °C, indicating that the NS successfully adsorbed onto the surfaces of the sodium bentonite, thus inhibiting the expansion of the sodium bentonite. As the NS concentration increased, the adsorption capacity of the NS increased.

3.2.5. SEM analysis

As shown in Fig. 14, the surface morphologies of the original shale and the shale sample after soaking in 3 wt% NS solution for 24 h were analyzed using SEM. It can be seen from the SEM images that the surface morphologies of the shale samples were significantly different before and after the NS modification. The surface of the original shale sample was very uneven. There were many small pores and micro-cracks that made water intrusion easier and caused the shale to expand and collapse. However, a smooth hydrophobic film was formed on the surface of the modified shale sample by adsorbing the NS, which changed the wettability of the shale and prevented the intrusion of water. The SEM images demonstrate that NS can effectively inhibit the dispersion of shale, thus maintaining its compressive strength (Fig. 5).

3.2.6. Scratch adhesion analysis

As shown in Fig. 15, the turning point occurs when the load reaches 47.55 N. When the load is less than 47.55 N, the indenter slides on the film surface, and the friction force changes linearly with increasing load. When the load reaches 47.55 N, an acoustic emission signal is generated, and the friction F between the indenter and the film substrate combination changes, indicating that the film and substrate begin to peel off. This experiment demonstrates that NS has a super adhesion ability, which can greatly enhance the adhesion between the NS and shale. This may be because its hydroxyl-containing structure is similar to the byssus protein secreted by marine mussels, which has an ultra-high

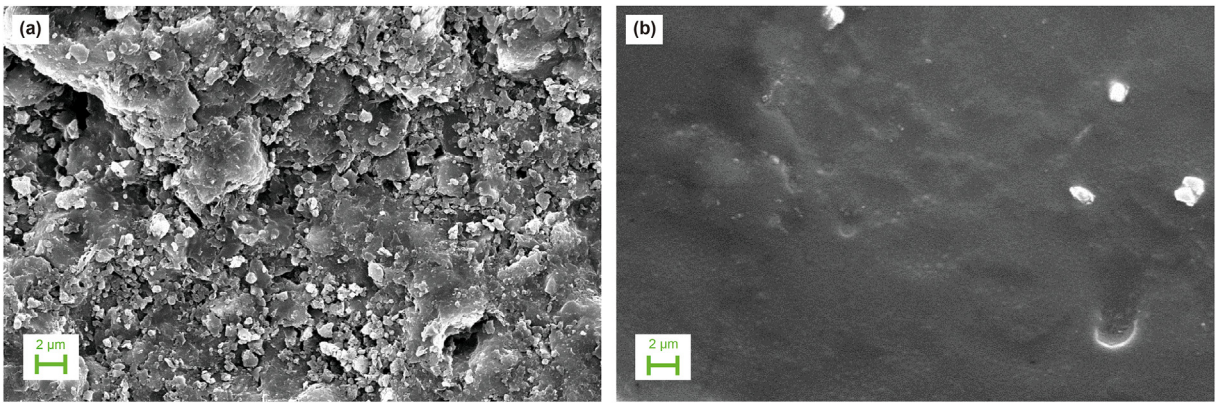

Fig. 14. SEM images of gas shale: (**a**) original shale and (**b**) shale after exposure to 3 wt% NS solution for 24 h.

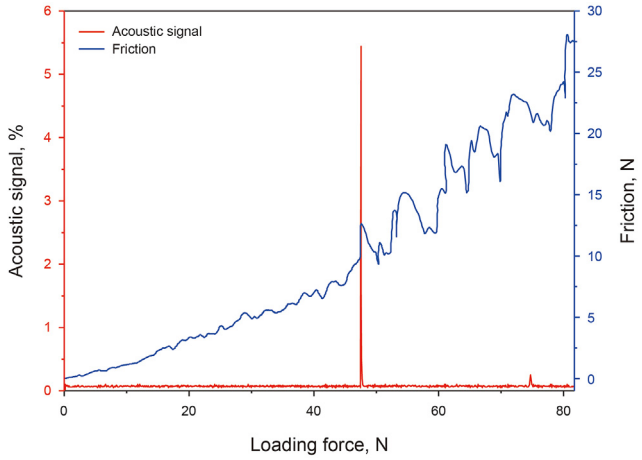

Fig. 15. The scratch adhesion test curve.

adhesion ability. Marine mussels attach to different underwater surfaces by using a series of proteins rich in 3,4-dihydroxyphenylalanine (DOPA). DOPA adheres to different substrates through hydrogen bond, metal catechol coordination, electrostatic interaction, cation π interaction and π-π aromatic interaction (Bandara et al., 2013; Li and Zeng, 2016). Through this type of adhesion, NS can enhance the binding force of the shale and reinforce the wellbore. This is consistent with the results of the compressive strength tests (Fig. 5).

Table 6
Effects of different inhibitors on the filtrate loss properties of the base-mud.

Additive	Condition	AV, mPa·s	PV, mPa·s	YP, Pa	API filtrate loss, mL
0	BHR	7	6	1	24.0
	AHR	9	8	1	26.0
1 wt% KCl	BHR	16	2	14	86.0
	AHR	12.5	3	9.5	67.2
1 wt% PA	BHR	18	1	17	216
	AHR	5	4	1	172
1 wt% NS	BHR	8.5	6	2.5	23.2
	AHR	11.5	9	2.5	20.8

3.2.7. Probable inhibition mechanism

Notoginsenoside (NS) is composed of hydrophilic and hydrophobic parts. The hydrophobic part is dammarane in triterpenoid saponins, and the hydrophilic part is mainly composed of polyhydroxy sugar chain residues. Adsorption experiments and FTIR show that the polyhydroxy groups in the hydrophilic part of the NS interact with the oxygen atoms on the clay surfaces to form multi-point adsorption via hydrogen bonding. And the SEM and contact angle measurements demonstrate that the hydrophobic part of the NS faces the water phase (Fig. 16), forming a hydrophobic film (Fig. 14), which inhibits the hydration of the clay by preventing the adsorption of water. This is consistent with the results of the mud ball experiments, the linear expansion and the recovery tests. In addition, its hydroxyl-containing structure is similar to that of the byssus protein secreted by marine mussel, which has an ultra-high adhesion ability compared with conventional inhibitors (Fig. 15).

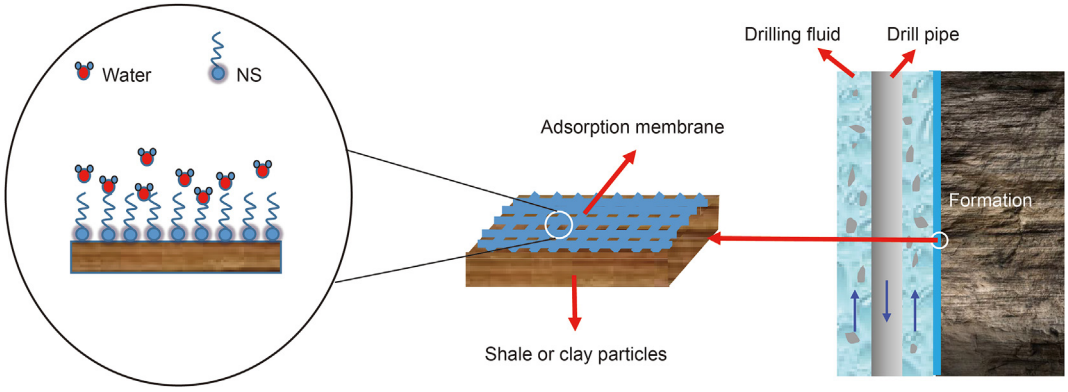

Fig. 16. The proposed inhibition mechanism of NS.

Table 4
Environmental indicator evaluation results.

Indicator	Measured value	Standard value	Classification
EC_{50}, mg/L	37800	≥30000	Nontoxic
BOD_5:COD, %	29.42	>25	Easily degradable

Table 5
Effects of NS concentration on the rheological and filtrate loss properties of the base-mud.

NS concentration, wt%	Condition	AV, mPa·s	PV, mPa·s	YP, Pa	API filtrate loss, mL
0	BHR	7	6	1	24.0
	AHR	9	8	1	26.0
0.5	BHR	8.5	6	2.5	23.8
	AHR	11	9	2	21.6
1	BHR	8.5	6	2.5	23.2
	AHR	11.5	9	2.5	20.8
2	BHR	9	6	3	20.8
	AHR	11.5	9	2.5	20.4

Table 7
Basic properties of drilling fluid systems.

NS concentration, wt%	ρ, g·cm^{-3}	Condition	AV, mPa·s	PV, mPa·s	YP, Pa	YP/PV, Pa/(mPa·s)	G'/G'', Pa	API filtrate loss, mL	HTHP filtrate loss, mL	Rate of recovery, %
0	1.03 (unweighted)	BHR	32.5	24	8.5	0.35	2.0/5.0	3.8	–	–
		AHR	36	25	11	0.44	2.0/5.5	3.6	20	71.25
0.5	1.03 (unweighted)	BHR	33.5	24	9.5	0.39	2.5/5.5	3.8	–	–
		AHR	39	26	13	0.50	2.5/6.0	3.4	19	98.25
0	1.5 (weighted)	BHR	45	33	12	0.36	2.5/6.0	3.2	–	–
		AHR	52.5	36	16.5	0.45	2.5/6.5	3.0	18	69.65
0.5	1.5 (weighted)	BHR	48	33	15	0.45	3.0/6.5	3.0	–	–
		AHR	56	37	19	0.51	3.5/7.0	2.8	16	97.85

Note: HTHP filtrate loss indicates filtrate loss measured under high temperature and high pressure.

This can be proved by the scratch adhesion test. Through adhesion, it can strengthen the wellbore, effectively maintaining the strength of the shale (Fig. 5) and stabilizing the wellbore. Therefore, the inhibition mechanism of NS is different from that of traditional inhibitors, which provides a new idea for the molecular design of inhibitors in the future (Ghasemi et al., 2019, Shadizadeh et al., 2015; Zhang et al., 2019).

3.3. Environmental aspects

To evaluate the environmental performance of NS, the EC_{50}, COD, and BOD_5 values of NS were measured according to the corresponding test standards. The EC_{50} value is 37,800, which is greater than 30,000. This indicates that NS is non-toxic. The BOD_5 is 303 and the COD is 1030. The BOD_5/COD is 29.42%, which is greater than 25%. This suggests that NS is easily degradable. The evaluation results (Table 4) show that as a natural surfactant, NS has the advantages of being non-toxic and biodegradable. This is particularly important for offshore drilling operations.

3.4. Formulation optimization and performance evaluation of drilling fluid

Table 5 shows the effects of the different concentrations of NS on the rheology and filtration of the base mud before hot rolling (BHR) and after hot rolling (AHR) at 120 °C. As the NS concentration increased, the viscosity of the drilling fluid slightly increased and the filtration rate gradually decreased. Table 6 shows that NS is more compatible than traditional inhibitors. Through the compatibility evaluation of the NS inhibitor and other common drilling fluid treatment agents, the ideal formulation for drilling fluid was determined to be as follows: water + 4 wt% bentonite + 0.1 wt% FA-367 + 0.5 wt% CMJ-2 + 0.5 wt% PAC-LV + 2 wt% NP-1 + 2 wt% emulsified asphalt + 0.5 wt% NS + 85 wt% barite. The drilling fluid has a good rheology, reduced filtration, a strong hydration inhibition ability, and a rolling recovery rate of 97.85% (Table 7) (Liu et al., 2019).

4. Conclusions

In this study, the application prospect of NS as a shale inhibitor was systematically investigated. NS can effectively inhibit the hydration of clay and stabilize the wellbore. The results of the inhibition evaluation show that NS is superior to conventional inhibitors such as KCl and polyamine (PA). When the NS molecules come in contact with the wellbore, the NS adsorbs onto the clay surface through hydrogen bonds to form a hydrophobic film, which prevents the entry of water molecules and effectively inhibits the hydration of the clay. In addition, its hydroxyl-containing structure has an ultra-high adhesion ability, which can enhance the binding force of shale and keep the strength of the shale unchanged. In addition, NS is nontoxic, environmentally friendly, and compatible with other treatment agents. As an efficient green shale water-based drilling fluid inhibitor, NS has broad application prospects.

Acknowledgments

This research was financially supported by the National Natural Science Foundation of China (Grants 51904328) and the Natural Science Foundation of China (Grants 52074330).

References

Aftab, A., Ali, M., Sahito, M.F., et al., 2020. Environmental friendliness and high performance of multifunctional tween 80/ZnO-nanoparticles-added water-based drilling fluid: an experimental approach. ACS Sustain. Chem. Eng. 8 (30), 11224–11243. https://doi.org/10.1021/acssuschemeng.0c02661.
Attar, F., Johannesson, T., 1996. Adhesion evaluation of thin ceramic coatings on tool steel using the scratch testing technique. Surf. Coating. Technol. 78 (1–3), 87–102. https://doi.org/10.1016/0257-8972(94)02396-4.
Bai, X., Wang, H., Luo, Y., et al., 2017. The structure and application of amine-terminated hyperbranched polymer shale inhibitor for water-based drilling fluid. J. Appl. Polym. Sci. 134 (46), 45466. https://doi.org/10.1002/app.45466.
Bandara, N., Zeng, H., Wu, J., 2013. Marine mussel adhesion: biochemistry, mechanisms, and biomimetics. J. Adhes. Sci. Technol. 27 (18–19), 2139–2162. https://doi.org/10.1080/01694243.2012.697703.
Boek, E., Coveney, P., Skipper, N., 1995. Monte Carlo molecular modeling studies of hydrated Li-, Na-, and K-smectites: understanding the role of potassium as a clay swelling inhibitor. J. Am. Chem. Soc. 117 (50), 12608–12617. https://pubs.acs.org/doi/pdf/10.1021/ja00155a025.
Bull, S., Berasetegui, E., 2006. An overview of the potential of quantitative coating adhesion measurement by scratch testing. Tribol. Int. 39 (2), 99–114. https://doi.org/10.1016/j.triboint.2005.04.013.
Cai, J., Chenevert, M.E., Sharma, M.M., et al., 2012. Decreasing water invasion into Atoka shale using nonmodified silica nanoparticles. SPE Drill. Complet. 27 (1), 103–112. https://doi.org/10.2118/146979-PA.
Chalker, P., Bull, S., Rickerby, D., 1991. A review of the methods for the evaluation of coating-substrate adhesion. Mater. Sci. Eng., A 140, 583–592. https://doi.org/10.1016/0921-5093(91)90482-3.
Chang, X., Sun, J., Xu, Z., et al., 2019. Synthesis of a novel environment-friendly filtration reducer and its application in water-based drilling fluids. Colloid. Surface. Physicochem. Eng. Aspect. 568, 284–293. https://doi.org/10.1016/j.colsurfa.2019.01.055.
Chen, G., Chenevert, M.E., Sharma, M.M., et al., 2003. A study of wellbore stability in shales including poroelastic, chemical, and thermal effects. J. Petrol. Sci. Eng. 38 (3–4), 167–176. https://doi.org/10.1016/S0920-4105(03)00030-5.
Chen, G., Yan, J., Lili, L., et al., 2017. Preparation and performance of amine-tartaric salt as potential clay swelling inhibitor. Appl. Clay Sci. 138, 12–16. https://doi.org/10.1016/j.clay.2016.12.039.
Chu, Q., Lin, L., Su, J., 2020. Amidocyanogen silanol as a high-temperature-resistant shale inhibitor in water-based drilling fluid. Appl. Clay Sci. 184, 105396. https://doi.org/10.1016/j.clay.2019.105396.
Chu, Q., Lin, L., Zhao, Y., 2019. Hyperbranched polyethylenimine modified with silane coupling agent as shale inhibitor for water-based drilling fluids. J. Petrol. Sci. Eng. 182, 106333. https://doi.org/10.1016/j.petrol.2019.106333.
Duan, L., Xiong, X., Hu, J., et al., 2017. Panax notoginseng saponins for treating coronary artery disease: a functional and mechanistic overview. Front. Pharmacol. 8, 702. https://doi.org/10.3389/fphar.2017.00702.
Dye, W., Daugereau, K., Hansen, N., et al., 2005. New water-based mud balances high-performance drilling and environmental compliance. In: SPE/IADC Drilling Conference. Society of Petroleum Engineers. https://doi.org/10.2118/92367-MS.
Edward, W.W., 1921. The dynamics of capillary flow. Phys. Rev. 17 (3), 273. https://doi.org/10.1103/PhysRev.17.273.
Estrada, J.M., Bhamidimarri, R., 2016. A review of the issues and treatment options

for wastewater from shale gas extraction by hydraulic fracturing. Fuel 182, 292–303. https://doi.org/10.1016/j.fuel.2016.05.051.
Friedheim, J., Guo, Q., Young, S., et al., 2011. Testing and evaluation techniques for drilling fluids-shale interaction and shale stability. In: Proceedings of 45th US Rock Mechanics/Geomechanics Symposium.
Fu, L., Liao, K., Ge, J., et al., 2020. Preparation and inhibition mechanism of bis-quaternary ammonium salt as shale inhibitor used in shale hydrocarbon production. J. Mol. Liq. 309, 113244. https://doi.org/10.1016/j.molliq.2020.113244.
Ghasemi, M., Moslemizadeh, A., Shahbazi, K., et al., 2019. Primary evaluation of a natural surfactant for inhibiting clay swelling. J. Petrol. Sci. Eng. 178, 878–891. https://doi.org/10.1016/j.petrol.2019.02.073.
Hoelscher, K.P., de Stefano, G., Riley, M., et al., 2012. Application of nanotechnology in drilling fluids. In: SPE International Oilfield Nanotechnology Conference and Exhibition. Society of Petroleum Engineers. https://doi.org/10.2118/157031-MS.
Huang, W., Li, X., Qiu, Z., et al., 2017. Inhibiting the surface hydration of shale formation using preferred surfactant compound of polyamine and twelve alkyl two hydroxyethyl amine oxide for drilling. J. Petrol. Sci. Eng. 159, 791–798. https://doi.org/10.1016/j.petrol.2017.10.006.
Huang, X., Shen, H., Sun, J., et al., 2018a. Nanoscale laponite as a potential shale inhibitor in water-based drilling fluid for stabilization of wellbore stability and mechanism study. ACS Appl. Mater. Interfaces 10 (39), 33252–33259. https://doi.org/10.1021/acsami.8b11419.
Huang, X., Sun, J., Lv, K., et al., 2018b. Application of core-shell structural acrylic resin/nano-SiO_2 composite in water based drilling fluid to plug shale pores. J. Nat. Gas Sci. Eng. 55, 418–425. https://doi.org/10.1016/j.jngse.2018.05.023.
Institute, A.P., 2009. Recommended Practice for Laboratory Testing of Drilling Fluids.
Ji, G., Sun, T., Zhou, Q., et al., 2002. Constructed subsurface flow wetland for treating heavy oil-produced water of the Liaohe Oilfield in China. Ecol. Eng. 18 (4), 459–465. https://doi.org/10.1016/S0925-8574(01)00106-9.
Jia, H., Huang, P., Wang, Q., et al., 2019. Investigation of inhibition mechanism of three deep eutectic solvents as potential shale inhibitors in water-based drilling fluids. Fuel 244, 403–411. https://doi.org/10.1016/j.fuel.2019.02.018.
Jiang, G., Yourong, Q., Yuxiu, A., et al., 2016. Polyethyleneimine as shale inhibitor in drilling fluid. Appl. Clay Sci. 127, 70–77. https://doi.org/10.1016/j.clay.2016.04.013.
Lal, M., 1999. Shale stability: drilling fluid Interaction and shale strength. In: SPE Asia Pacific Oil and Gas Conference and Exhibition. Society of Petroleum Engineers. https://doi.org/10.2118/54356-MS.
Li, L., Zeng, H., 2016. Marine mussel adhesion and bio-inspired wet adhesives. Biotribology 5, 44–51. https://doi.org/10.1016/j.biotri.2015.09.004.
Li, W., Liu, J., Zhao, X., et al., 2019. Development and screening of additives for biodiesel based drilling fluids: principles, strategies and experience. In: SPE International Conference on Oilfield Chemistry. Society of Petroleum Engineers. https://doi.org/10.2118/193597-MS.
Li, W., Zhao, X., Ji, Y., et al., 2016a. Investigation of biodiesel-based drilling fluid, Part 1: biodiesel evaluation, invert-emulsion properties, and development of a novel emulsifier package. SPE J. 21 (5), 1755–1766. https://doi.org/10.2118/180918-PA.
Li, W., Zhao, X., Ji, Y., et al., 2016b. Investigation of biodiesel-based drilling fluid, Part 2: formulation design, rheological study, and laboratory evaluation. SPE J. 21 (5), 1767–1781. https://doi.org/10.2118/180926-PA.
Li, W., Zhao, X., Li, Y., et al., 2015. Laboratory investigations on the effects of surfactants on rate of penetration in rotary diamond drilling. J. Petrol. Sci. Eng. 134, 114–122. https://doi.org/10.1016/j.petrol.2015.07.027.
Liu, J., Dai, Z., Li, C., et al., 2019. Inhibition of the hydration expansion of Sichuan gas shale by adsorption of compounded surfactants. Energy Fuel. 33 (7), 6020–6026. https://doi.org/10.1021/acs.energyfuels.9b00637.
Liu, X., Liu, K., Gou, S., et al., 2014. Water-soluble acrylamide sulfonate copolymer for inhibiting shale hydration. Ind. Eng. Chem. Res. 53 (8), 2903–2910. https://doi.org/10.1021/ie403956d.
Lv, K., Huang, X., Li, H., et al., 2020. Modified biosurfactant cationic alkyl polyglycoside as an effective additive for inhibition of highly reactive shale. Energy Fuel. 34 (2), 1680–1687. https://doi.org/10.1021/acs.energyfuels.9b04131.
Moslemizadeh, A., Aghdam, SK-y, Shahbazi, K., et al., 2016. Assessment of swelling inhibitive effect of CTAB adsorption on montmorillonite in aqueous phase. Appl. Clay Sci. 127, 111–122. https://doi.org/10.1016/j.clay.2016.04.014.
O'Brien, D.E., Chenevert, M.E., 1973. Stabilizing sensitive shales with inhibited, potassium-based drilling fluids. J. Petrol. Technol. 25 (9), 1089–1100. https://doi.org/10.2118/4232-PA.
Pašić, B., Gaurina Međimurec, N., Matanović, D., 2007. Wellbore instability: causes and consequences. Rudarsko-Geolosko-Naftni Zb. 19 (1), 87–98. https://hrcak.srce.hr/19296.
Patel, A., Stamatakis, S., Young, S., et al., 2007. Advances in inhibitive water-based drilling fluids—can they replace oil-based muds?. In: International Symposium on Oilfield Chemistry. Society of Petroleum Engineers. https://doi.org/10.2118/106476-MS.
Peng, B., Luo, P.Y., Guo, W.Y., et al., 2013. Structure–property relationship of polyetheramines as clay-swelling inhibitors in water-based drilling fluids. J. Appl. Polym. Sci. 129 (3), 1074–1079. https://doi.org/10.1002/app.38784.
Pi, Y., Zheng, Z., Bao, M., et al., 2015. Treatment of partially hydrolyzed polyacrylamide wastewater by combined Fenton oxidation and anaerobic biological processes. Chem. Eng. J. 273, 1–6. https://doi.org/10.1016/j.cej.2015.01.034.
Qu, J., Xu, N., Zhang, J., et al., 2020. Panax notoginseng saponins and their applications in nervous system disorders: a narrative review. Ann. Transl. Med. 8 (22), 1525. https://doi.org/10.21037/atm-20-6909.
Qu, Y., Lai, X., Zou, L., et al., 2009. Polyoxyalkyleneamine as shale inhibitor in water-based drilling fluids. Appl. Clay Sci. 3 (44), 265–268. https://doi.org/10.1016/j.clay.2009.03.003.
Razali, S., Yunus, R., Rashid, S.A., et al., 2018. Review of biodegradable synthetic-based drilling fluid: progression, performance and future prospect. Renew. Sustain. Energy Rev. 90, 171–186. https://doi.org/10.1016/j.rser.2018.03.014.
Salkuyeh, Y.K., Adams II, T.A., 2015. A novel polygeneration process to co-produce ethylene and electricity from shale gas with zero CO_2 emissions via methane oxidative coupling. Energy Convers. Manag. 92, 406–420. https://doi.org/10.1016/j.enconman.2014.12.081.
Shadizadeh, S.R., Moslemizadeh, A., Dezaki, A.S., 2015. A novel nonionic surfactant for inhibiting shale hydration. Appl. Clay Sci. 118, 74–86. https://doi.org/10.1016/j.clay.2015.09.006.
Spisak, B.J., 2011. Using Nanoparticle Stabilized Foam to Achieve Wellbore Stability in Shales. Ph.D. dissertation. The University of Texas at Austin. http://hdl.handle.net/2152/ETD-UT-2011-08-4327.
Tabak, A., Afsin, B., Caglar, B., et al., 2007. Characterization and pillaring of a Turkish bentonite (Resadiye). J. Colloid Interface Sci. 313 (1), 5–11. https://doi.org/10.1016/j.jcis.2007.02.086.
Talabani, S., Chukwu, G., Hatzignatiou, D., 1993. Drilling successfully through deforming shale formations: Case histories. In: Low Permeability Reservoirs Symposium. Society of Petroleum Engineers. https://doi.org/10.2118/25867-MS.
Uzayisenga, R., Ayeka, P.A., Wang, Y., 2014. Anti-diabetic potential of Panax notoginseng saponins (PNS): a review. Phytother Res. 28 (4), 510–516. https://doi.org/10.1002/ptr.5026.
van Oort, E., Lee, J., Friedheim, J., et al., 2004. New flat-rheology synthetic-based mud for improved deepwater drilling. In: SPE Annual Technical Conference and Exhibition. Society of Petroleum Engineers. https://doi.org/10.2118/90987-MS.
Wang, C.-Z., McEntee, E., Wicks, S., et al., 2006. Phytochemical and analytical studies of panax notoginseng (Burk.) FH chen. J. Nat. Med. 60 (2), 97–106. https://doi.org/10.1007/s11418-005-0027-x.
Wang, T., Guo, R., Zhou, G., et al., 2016. Traditional uses, botany, phytochemistry, pharmacology and toxicology of Panax notoginseng (Burk.) FH Chen: a review. J. Ethnopharmacol. 188, 234–258. https://doi.org/10.1016/j.jep.2016.05.005.
Wei, B., Li, Q., Jin, F., et al., 2016. The potential of a novel nanofluid in enhancing oil recovery. Energy Fuel. 30 (4), 2882–2891. https://doi.org/10.1021/acs.energyfuels.6b00244.
Xu, C., Wang, W., Wang, B., et al., 2019. Analytical methods and biological activities of Panax notoginseng saponins: recent trends. J. Ethnopharmacol. 236, 443–465. https://doi.org/10.1016/j.jep.2019.02.035.
Xu, J.-G., Qiu, Z., Zhao, X., et al., 2017. Hydrophobic modified polymer based silica nanocomposite for improving shale stability in water-based drilling fluids. J. Petrol. Sci. Eng. 153, 325–330. https://doi.org/10.1016/j.petrol.2017.04.013.
Xuan, Y., Jiang, G., Li, Y., et al., 2013. Inhibiting effect of dopamine adsorption and polymerization on hydrated swelling of montmorillonite. Colloid. Surface. Physicochem. Eng. Aspect. 422, 50–60. https://doi.org/10.1016/j.colsurfa.2013.01.038.
Yang, L., Jiang, G., Shi, Y., et al., 2017. Application of ionic liquid and polymeric ionic liquid as shale hydration inhibitors. Energy Fuel. 31 (4), 4308–4317. https://doi.org/10.1021/acs.energyfuels.7b00272.
Yang, X., Xiong, X., Wang, H., et al., 2014. Protective effects of panax notoginseng saponins on cardiovascular diseases: a comprehensive overview of experimental studies. Evid. base Compl. Alternative Med. 2014, 204840. https://doi.org/10.1155/2014/204840.
Yu, M., Chenevert, M.E., Sharma, M.M., 2003. Chemical–mechanical wellbore instability model for shales: accounting for solute diffusion. J. Petrol. Sci. Eng. 38 (3–4), 131–143. https://doi.org/10.1016/S0920-4105(03)00027-5.
Zhang, F., Sun, J., Chang, X., et al., 2019. A novel environment-friendly natural extract for inhibiting shale hydration. Energy Fuel. 33 (8), 7118–7126. https://doi.org/10.1021/acs.energyfuels.9b01166.
Zhang, X., Wei, B., Shang, J., et al., 2018. Alterations of geochemical properties of a tight sandstone reservoir caused by supercritical CO_2-brine-rock interactions in CO_2-EOR and geosequestration. J. CO_2 Utiliz. 28, 408–418. https://doi.org/10.1016/j.jcou.2018.11.002.
Zhang, Y., Zheng, J., Zheng, L., et al., 2015. Effect of adsorption time on the adhesion strength between salivary pellicle and human tooth enamel. J. Mech. Behav. Biomed. Mater. 42, 257–266. https://doi.org/10.1016/j.jmbbm.2014.11.024.
Zhong, H., Qiu, Z., Huang, W., et al., 2014. The development and application of a novel polyamine water-based drilling fluid. Petrol. Sci. Technol. 32 (4), 497–504. https://doi.org/10.1080/10916466.2011.592897.
Zhong, H., Qiu, Z., Tang, Z., et al., 2016. Study of 4, 4'-methylenebis-cyclohexanamine as a high temperature-resistant shale inhibitor. J. Mater. Sci. 51 (16), 7585–7597. https://doi.org/10.1007/s10853-016-0037-y.